iScience

CellPress
OPEN ACCESS

Article

Light-driven ammonium oxidation to dinitrogen gas by self-photosensitized biohybrid anammox systems

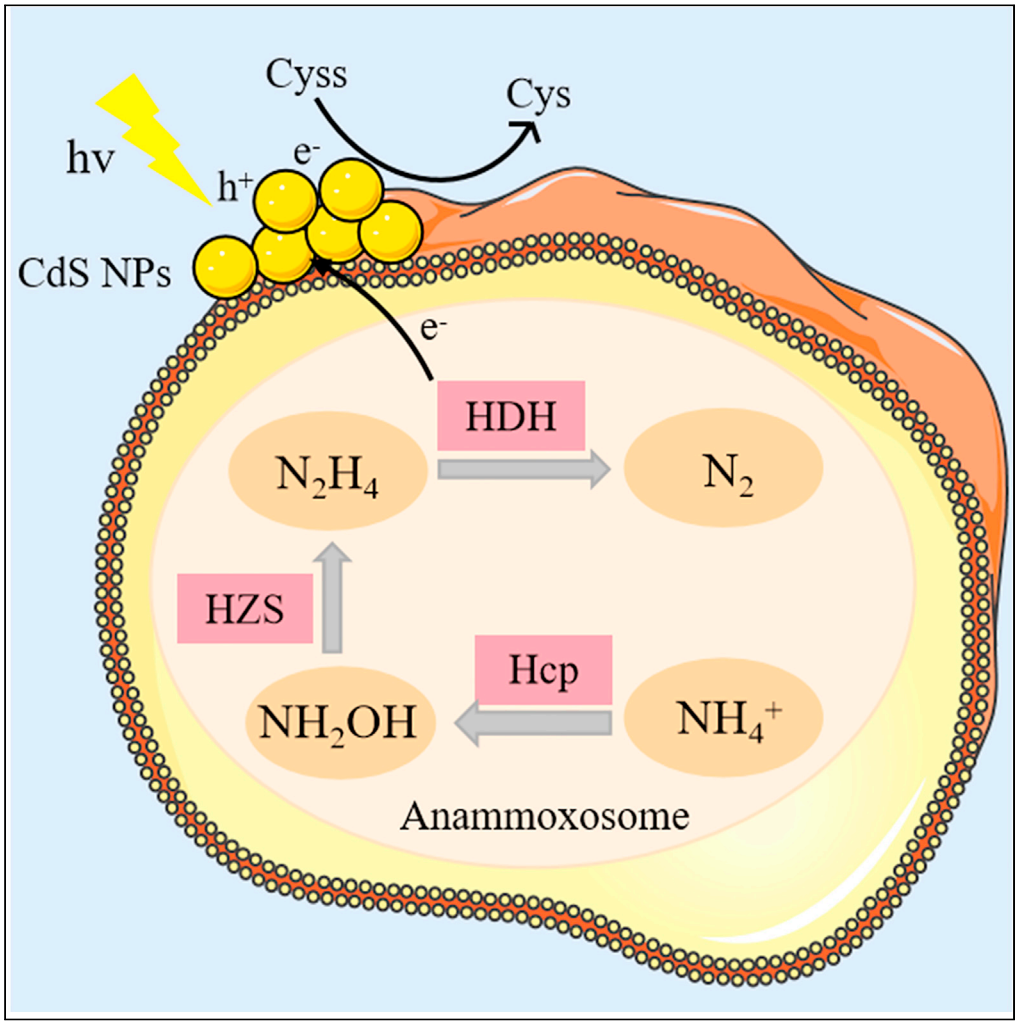

Meiwei Guo, Chao Wang, Sen Qiao

qscyj@mail.dlut.edu.cn

Highlights

An anammox-CdS biohybrid system were firstly constructed

The anammox-CdS system can utilize photoexcited holes to directly oxide NH_4^+ to N_2

NH_2OH was the intermediate rather than NO in the light-driven of NH_4^+ oxidation process

Guo et al., iScience 26, 106725
May 19, 2023
https://doi.org/10.1016/j.isci.2023.106725

iScience

CellPress
OPEN ACCESS

Article

Light-driven ammonium oxidation to dinitrogen gas by self-photosensitized biohybrid anammox systems

Meiwei Guo,[1] Chao Wang,[1] and Sen Qiao[1,2,*]

SUMMARY

The anaerobic ammonium oxidation (anammox) process exerts a very vital role in the global nitrogen cycle (estimated to contribute 30%–50% N_2 production in the oceans) and presents superiority in water/wastewater nitrogen removal performance. Until now, anammox bacteria can convert ammonium (NH_4^+) to dinitrogen gas (N_2) with nitrite (NO_2^-), nitric oxide (NO), and even electrode (anode) as electron acceptors. However, it is still unclear whether anammox bacteria could utilize photoexcited holes as electron acceptors to directly oxide NH_4^+ to N_2. Here, we constructed an anammox-cadmium sulfide nanoparticles (CdS NPs) biohybrid system. The photoinduced holes from the CdS NPs could be utilized by anammox bacteria to oxidize NH_4^+ to N_2. ^{15}N-isotope labeling experiments demonstrated that NH_2OH instead of NO was the real intermediate. Metatranscriptomics data further proved a similar pathway for NH_4^+ conversion with anodes as electron acceptors. This study provides a promising and energy-efficient alternative for nitrogen removal from water/wastewater.

INTRODUCTION

Nitrogen (N) is the necessary microelement for all organisms and is of significance to support their growth and normal metabolisms. However, diet structure change accompanied by the enhanced living standard will undoubtedly lead to much more protein intake than before by human beings. Consequently, more N-related pollutants, such as organic nitrogen and ammonium (NH_4^+), will further increase the processing load in sewage systems. For instance, the average nitrogen removal energy by the traditional biological nitrification-denitrification process was widely believed to be around ~2.6–6.2 kWh/kg N,[1] which is typically energy intensive. The energy of biological ammonium conversion to dinitrogen gas approximately occupies ~21.5%–51.2% of the energy (kWh/kg N) that is used to convert dinitrogen gas to ammonium in the industry (12.1 kWh/kg NH_3-N).[2,3] Besides the required energy, another main drawback is the production of nitrous oxide (N_2O), which is a potent greenhouse gas and is a 300-fold stronger greenhouse effect than CO_2.[4]

Thus, in order to reduce the energy and cost consumption of conventional nitrification-denitrification process, novel technologies have been developed in recent three decades, e.g., partial nitrification-denitrification process,[5] anaerobic ammonium oxidation (anammox) process,[6] and denitrifying anaerobic methane oxidation process.[7] Among them, anammox has attracted more attention, since it can directly oxidize ammonium with nitrite as electron acceptors anaerobically, as shown in Equation 1. It demonstrated no aeration and external carbon required compared to the traditional biological nitrification-denitrification process. Until now, there have been over 100 full-scale anammox applications worldwide.[4] Since wastewater usually contains organic nitrogen and ammonium compounds, the anammox process requires partial nitrification (transfer partial NH_4^+ to NO_2^-) to provide substrates. However, the selective inhibition of nitrite-oxidizing bacteria is complex and running-system dependent. Therefore, full-scale partial nitrification-anammox implements have been mainly for high ammonium concentration wastewater under mesophilic temperatures conditions, such as the side stream of digestate or some kind of industrial wastewater.[8,9] Moreover, according to Equation 1, further polishing is necessary in order to remove the generated NO_3^- by the anammox process itself, e.g., the traditional denitrification process.

$$NH_4^+ + 1.32NO_2^- + 0.066HCO_3^- + 0.13H^+ \rightarrow 1.02N_2 + 0.26NO_3^- + 0.066CH_2O_{0.5}N_{0.15} + 2.03H_2O \quad \text{(Equation 1)}$$

[1]Key Laboratory of Industrial Ecology and Environmental Engineering (Ministry of Education, China), School of Environmental Science and Technology, Dalian University of Technology, Dalian 116024, P.R. China

[2]Lead contact

*Correspondence: qscyj@mail.dlut.edu.cn

https://doi.org/10.1016/j.isci.2023.106725

Recently, promising research first demonstrated that anammox bacteria could oxide NH_4^+ to N_2 with the electrode as electron acceptors, via hydroxylamine (NH_2OH) as the intermediate.[10] According to the above study, anammox bacteria use OH^- ions from H_2O to form NH_2OH by oxidizing NH_4^+ firstly. Then, NH_4^+ reacts with NH_2OH to generate N_2H_4 as another intermediate. Finally, N_2H_4 decomposes into N_2 and hydrogen ions.[10] The proposed reactions of the electro-anammox were as following Equations 2–5[10]:

$$NH_4^+ + H_2O \rightarrow NH_2OH + 3H^+ + 2e^- \quad \text{(Equation 2)}$$

$$NH_4^+ + NH_2OH \rightarrow N_2H_4 + H_2O + H^+ \quad \text{(Equation 3)}$$

$$N_2H_4 \rightarrow N_2 + 4H^+ + 4e^- \quad \text{(Equation 4)}$$

$$2NH_4^+ \xrightarrow{+0.6\ V\ vs\ SHE} N_2 + 8H^+ + 6e^- \quad \text{(Equation 5)}$$

Furthermore, Sakimoto and colleagues have developed a more pioneered approach, which constructed a biohybrid system by combining photosensitizing non-photosynthetic microbes with self-precipitated metal semiconductor nanoparticles.[11] The synthesized metal semiconductor cadmium sulfide (CdS) nanoparticles are excellent candidates for light harvesters in biohybrids due to their tunable band gaps, rich surface-binding sites, excellent extinction coefficients, and favorable conduction/valence band energies.[12,13] In the above research, light harvesting semiconductors of CdS were biosynthesized by *Moorella thermoacetica* to generate acetate from CO_2, while cysteine was used as the sacrificial electron donor simultaneously.[11] Inspired by this research, many similar semiconductor biohybrid systems have recently been evolved, namely for light-driven CO_2 reduction,[14,15] light-driven hydrogen production,[16,17] and light-driven nitrogen fixation.[18] The chosen microbes are selected to take up the resultant charge from the inorganic material via various extracellular electron transfers pathways and perform the requisite complex catalytic chemistry through their evolved metabolic pathways, ideally generating products of high value at industrially relevant throughputs.[19] Notwithstanding only the utilization of photoexcited electrons was targeted and studied in the above reported research, and the utilization of photoexcited holes by non-photosynthetic microbes seemed to be completely ignored. Ren et al. rationally deduced that nano-semiconductor would also interact with anammox consortia by constructing phototroph-anammox symbiotic nitrogen removal system.[20] Based on the previous studies, we hypothesize that anammox bacteria might be able to utilize photoexcited holes as electron acceptors (similar to anodes as electron acceptors) to carry out the oxidation of NH_4^+ to N_2. To the best of our knowledge, there is no related study reported until now.

Therefore, we construct the anammox-CdS biohybrid system to investigate whether anammox bacteria can directly oxidize NH_4^+ to N_2 gas by utilizing photoexcited holes as electron acceptors in this study. A series of experiments were carried out to testify to the possibility of the above hypothesis. The ammonium oxidation efficiency of the constructed biohybrid systems was systematically explored and up to 80%, and the underlying reason for N_2 production was investigated in detail. In the end, the possible mechanism of anammox bacteria utilizing photoexcited holes was also extensively evaluated.

RESULTS

Species and contents of anammox bacteria in the UASB reactor

Fluorescence *in situ* hybridization analysis of the upflow anaerobic sludge bed (UASB) reactor enrichment was shown in Figure S1. Among them, the blue color (from DAPI) represented the total bacteria (Figure S1A), and the red color (from the Cy3 fluorophore of Amx368 probe) represented anammox bacteria (Figure S1B). In the field of view, anammox bacteria appeared rose red color due to its binding to both the probe and DAPI (Figure S1C). From Figure S1C, anammox bacteria were evenly distributed in the UASB reactor enrichment with high abundance. To quantify the abundance of anammox bacteria in the UASB reactor enrichment, ImageJ (+64-bit Java 1.8.0_172) was further used to count anammox bacteria and total bacteria, and the average abundance of anammox bacteria was estimated to be about 70%. And 16S rRNA analysis further illustrated that *Candidatus Kuenenia stuttgartiensis* and *Candidatus Brocadia anammoxidans* were the dominant species in the enrichment (Figure S2).

Characterization of the biohybrid systems

Until now, only several kinds of nano-semiconductors were reported to successfully construct biohybrid systems, among which CdS was one of the most popular visible-light harvesting materials due to its

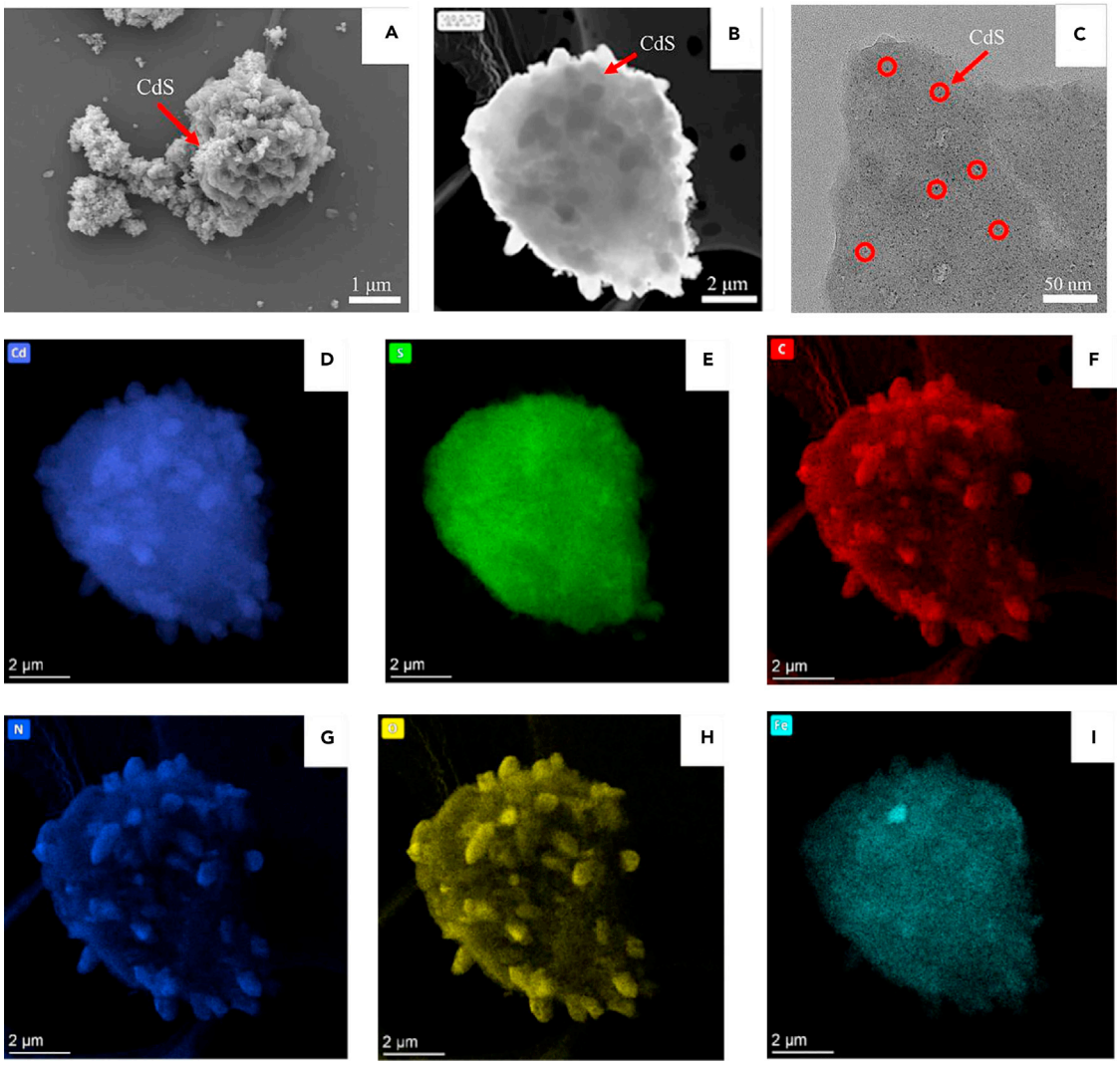

Figure 1. Electron microscopy of the anammox-CdS biohybrid system

(A) HR-SEM image of CdS nanoparticles on the surface of anammox biomass.

(B) HAADF TEM image of anammox-CdS biohybrid system.

(C) TEM image of CdS nanoparticles attaching to anammox bacterial surfaces.

(D–I) EDS mapping images of anammox bacteria surfaces mainly composed of cadmium, sulfur, carbon, nitrogen, oxygen, and iron.

attractive photocatalytic properties and relatively narrow band gap (2.39 eV).[17,21] The microbial-CdS biohybrid system demonstrated CO_2-to-fuel, H_2 production, and N_2 fixation results combined with different microbes, including *M. thermoacetica, Desulfovibrio desulfuricans, Shewanella oneidensis, Rhodopseudomonas palustris*, etc.[11,17] Thus, CdS nanoparticles were chemically synthesized and mixed with anammox biomass for over 24 h in order to make them blend completely. The CdS nanoparticles were proved to be responsive to visible light ($\lambda > 420$ nm) by UV-vis absorption spectrum (UV-Vis, UH41500304042501, Hitachi, Japan) and Congo red photocatalytic degradation (Figures S3 and S4) and composed of Cd and S elements based on the observation by an X-ray photoelectron spectrometer (XPS, ESCALAB XI+, Thermo Fisher Scientific, USA) (Figure S5). The peaks located at 412, 405, and 162 eV were assigned to Cd $3d_{2/2}$, Cd $3d_{5/2}$, and S 2p, respectively, which indicated the existence of CdS. Ultra-high resolution field emission scanning electron microscope (HR-SEM, JSM-7900F, Hitachi, Japan), transmission electron microscopy of high-angle annular dark field (HAADF TEM, SUPER X, FEI, USA), and transmission electron microscopy (TEM, SUPER X, FEI, USA) observation clearly demonstrated that high intensity of CdS nanoparticles anchored on the surface of anammox bacteria cells (Figures 1A–1C). Energy dispersive X-ray spectroscopy

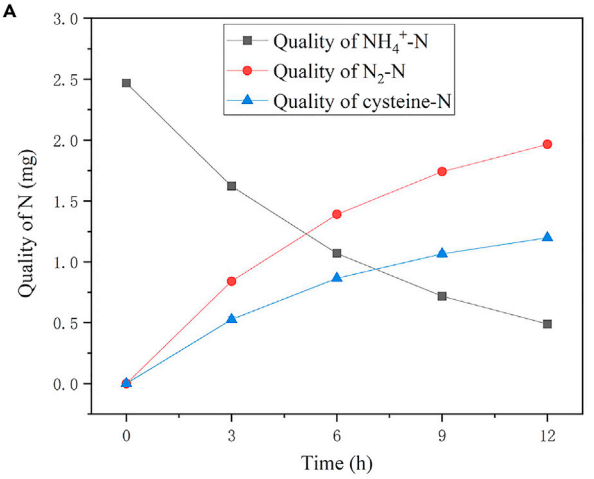
A
Quality of NH_4^+-N
Quality of N_2-N
Quality of cysteine-N
Quality of N (mg)
Time (h)
0.0
0.5
1.0
1.5
2.0
2.5
3.0
0
3
6
9
12

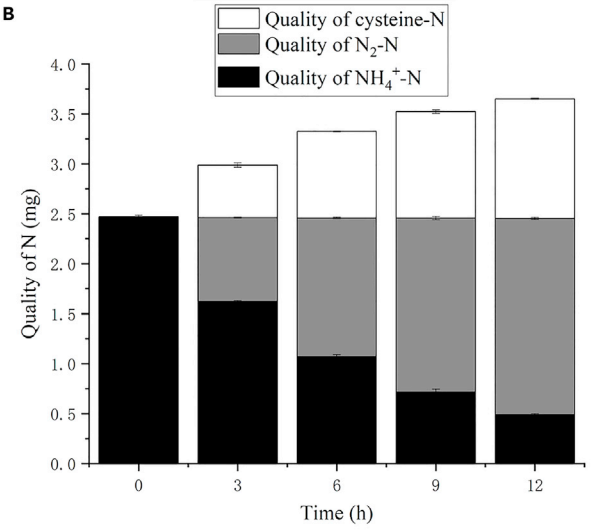
B
Quality of cysteine-N
Quality of N_2-N
Quality of NH_4^+-N
Quality of N (mg)
Time (h)
0.0
0.5
1.0
1.5
2.0
2.5
3.0
3.5
4.0
0
3
6
9
12

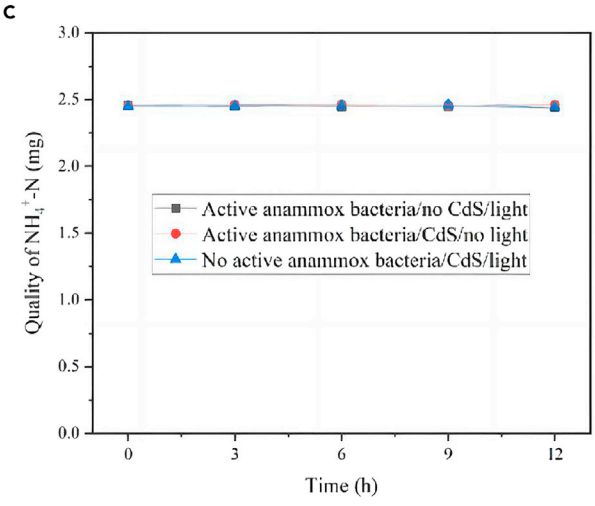
C
Active anammox bacteria/no CdS/light
Active anammox bacteria/CdS/no light
No active anammox bacteria/CdS/light
Quality of NH_4^+-N (mg)
Time (h)
0.0
0.5
1.0
1.5
2.0
2.5
3.0
0
3
6
9
12

Figure 2. Photocatalytic activity of the anammox-CdS biohybrid system

The anammox-CdS biohybrid system irradiated at an LED lamp (490 nm) was fed with 25 mg-N/L NH_4^+ and 0.1 g cystine.

(A) Removal of NH_4^+ and production of N_2 and cysteine over time.

(B) The balance of total nitrogen including NH_4^+-N, cysteine-N, and N_2-N.

(C) NH_4^+ variations in three control groups with active anammox bacteria/no CdS/light, with active anammox bacteria/CdS/no light, and with no active anammox bacteria/CdS/light. All the results were the average of tri-measurements with standard error.

(EDS, Hitachi, Japan) mapping further revealed that the anammox-CdS biohybrid systems consisted of Cd, S, C, N, O, and Fe elements, in which the latter four elements came from microorganisms obviously (Figures 1D–1I). X-ray diffractometer analysis (XRD, D8 Advance, Bruker, Germany) (Figure S6) confirmed the diffraction pattern and further the crystalline nature of the synthesized CdS nanoparticles, which was consistent with that of CdS cubic structures (standard card JCPDS card no. 80-0019).

Ammonium oxidation profile

To prove the applicability of the anammox-CdS biohybrid system, photocatalytic NH_4^+ oxidation experiments were carried out. Figure 2A confirmed NH_4^+ removal from the anammox-CdS biohybrid system under visible light (>420 nm, 9.72 mW/cm^2) irradiation. Within 12 h reaction, NH_4^+-N concentration decreased from 2.5 to 0.5 mg, indicating a removal efficiency of 80%. Simultaneously, N_2 productions were observed from the very beginning and finally increased to 2.0 mg and cysteine generations were also monitored with a similar increasing trend as N_2. As expected, cysteine was generated from cystine, which quenched photoexcited electrons as the sacrifice. Figure 2B presented the N balance profiles during the whole experiment. The total nitrogen (TN) amount did not keep stale, albeit appeared to increase with reaction time. With further analysis, the increased part of TN could be ascribed to the N amount included in cysteine in which the contained two N atoms would interfere with the NH_4^+-N analysis results and further lead to the TN amount increase. Without considering cysteine interference, the TN amount of N_2 + NH_4^+ was kept a good balance, as shown in Figure 2B. Figure 2C showed the effect of three control groups on photocatalytic NH_4^+ oxidation. There were the control 1 with active anammox bacteria and light but no CdS nanoparticles (NPs), the control 2 with active anammox bacteria and CdS NPs but no light, and the control 3 with light and CdS NPs but no active anammox bacteria. As shown in Figure 2C, the NH_4^+-N concentrations in all three controls were kept very stable as the initial, while NH_4^+-N concentrations in the experimental group appeared a clear decrease trend. These results illustrated that light, active anammox bacteria and CdS NPs were necessary components for NH_4^+-N removal in our light-driven NH_4^+ removal process. Moreover, real-time PCR analysis demonstrated that anammox bacteria could grow dependent on NH_4^+ and photoexcited holes in the biohybrid system with a growth rate of 0.044 days^{-1} (doubling time = 22.7 days, Table S1).

Molecular mechanism of photocatalytic-dependent anammox pathway

After verifying that anammox biomass was photocatalytic active, isotope labeling experiments were implemented to further exploit how NH_4^+ was converted to N_2 by the anammox-CdS biohybrid system. In this scenario, $^{15}NH_4^+$ was used as the sole N source and substrate for anammox biomass instead of $^{14}NH_4^+$. In order to avoid the destruction of the anammox-CdS biohybrid system, only liquid supernatant was poured out from the vials before isotope labeling $^{15}NH_4^+$ addition. Thus, both the residual $^{14}NH_4^+$ and the added $^{15}NH_4^+$ could react with the residual $^{14}NO_2^-$ via normal anammox reaction to produce $^{28}N_2$ and $^{29}N_2$, respectively, as shown in Figure 3. Synchronously, $^{30}N_2$ production was also detected with a quite high level compared to both $^{28}N_2$ and $^{29}N_2$ from the very beginning of the experiments. Due to the low levels of the residual $^{14}NH_4^+$ and $^{14}NO_2^-$, both of them were soon consumed only after 3 h reaction. Whereafter, a steady increase of $^{30}N_2$ was continuously observed during the follow-up experiment. These results further verified that NH_4^+ could be converted to N_2 by anammox biomass with photoexcited holes as sole electron acceptors.

Kartal et al. proposed a set of three redox reactions (Equations 6–8) involving N_2H_4 and nitric oxide (NO) as the intermediates to explain the overall anammox stoichiometry (Equation 9), which were based on a series of analyses of the anammox bacterium *Candidatus K. stuttgartiensis*.[22] Oshiki et al. explored the molecular mechanism of the anammox bacterium "*Candidatus Brocadia sinica*" and demonstrated that "*Candidatus B. sinica*" could reduce NO_2^- to NH_2OH, instead of NO, with as yet unidentified nitrite reductase.[23] Shaw et al. suggested that NH_2OH, instead of NO, was an intermediate of the electrode-dependent anammox process, which exploited ammonium oxidation of *Candidatus Scalindua*, *Candidatus Brocadia*, and

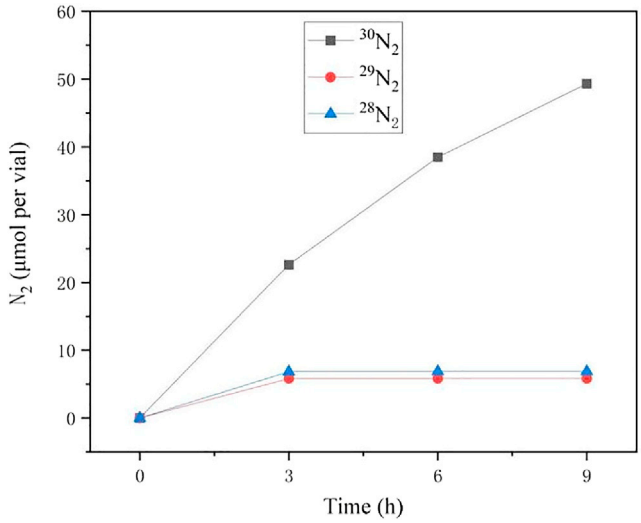

Figure 3. Time course of the anaerobic oxidation of $^{15}NH_4^+$ to $^{28}N_2$, $^{29}N_2$, and $^{30}N_2$

The anammox-CdS biohybrid system was added 25 mg-N/L $^{15}NH_4^+$ under the irradiation of an LED lamp (490 nm). $^{30}N_2$ was produced by the $^{15}NH_4^+$ oxidation, production of $^{29}N_2$ was synthesized from $^{15}NH_4^+$ and the residual $^{14}NO_2^-$ in the sample, and $^{28}N_2$ was produced by a trace amount of $^{14}NH_4^+$ and $^{14}NO_2^-$.

Candidatus K. stuttgartiensis with anodes as the only electrons acceptors.[10] Therefore, both possibilities of NH_2OH and NO as the intermediate were explored in our scenario. Similarly, 2-phenyl-4,4,5,5,-tetramethylimidazoline-1-oxyl-3-oxide (PTIO) was used as the NO scavenger to investigate whether NO was the intermediate of the photocatalytic-anammox process. The normal anammox process with NH_4^+ and NO_2^- as the substrate was severely hindered with PTIO addition, and ammonium concentration did not reduce anymore during the whole reaction period (Figure S7A). While no any inhibitory impact was observed in the photocatalytic experimental vials with PTIO addition, as shown in Figure S7B. The PTIO experiments proved NO not the real intermediate during the photocatalytic-anammox process.

$$NO_2^- + 2H^+ + e^- \rightarrow NO + H_2O \ (E_0' = +0.38V) \quad \text{(Equation 6)}$$

$$NO + NH_4^+ + 2H^+ + 3e^- \rightarrow N_2H_4 + H_2O \ (E_0' = +0.06V) \quad \text{(Equation 7)}$$

$$N_2H_4 \rightarrow N_2 + 4H^+ + 4e^- \ (E_0' = -0.75V) \quad \text{(Equation 8)}$$

$$NH_4^+ + NO_2^- \rightarrow N_2 + 2H_2O \ (\Delta G^{o'} = -357\ kJ/mol) \quad \text{(Equation 9)}$$

On the other hand, $^{15}NH_4^+$ (25 mg-N/L) and $^{14}NH_2OH$ (12.5 mg-N/L) were added into the anammox-CdS biohybrid systems to exploit whether NH_2OH was the intermediate during the photocatalytic NH_4^+-N oxidation process by anammox biomass. As our hypothesis, anammox bacteria would preferentially convert $^{14}NH_2OH$ and $^{15}NH_4^+$ to produce $^{29}N_2$. Simultaneously, the photocatalytic $^{15}NH_4^+$ oxidation led to the accumulation of $^{15}NH_2OH$, which reacted with $^{15}NH_4^+$ further to generate $^{30}N_2$. Figure 4 confirmed the generation of both $^{29}N_2$ and $^{30}N_2$ as our expectation. The above isotope experiments implied that NH_2OH, instead of NO in the normal anammox reaction, was the real intermediate during the photocatalytic NH_4^+-N oxidation process by anammox biomass.

Metatranscriptomic analysis of the anammox-CdS biohybrid system

To understand the possible metabolic pathways in response to the photoexcited holes-dependent ammonium oxidation to nitrogen, the transcriptomic alternation was analyzed by comparing the photocatalytic-anammox process with the normal anammox process (Figure 5). Since the level of mRNA cannot proportionally reflect the expression of the protein they encode, it is very difficult to accurately forecast the protein function and activity only according to quantitative transcriptome results. Therefore, the following discussion from metatranscriptomic data analysis is our assumption. When it was under

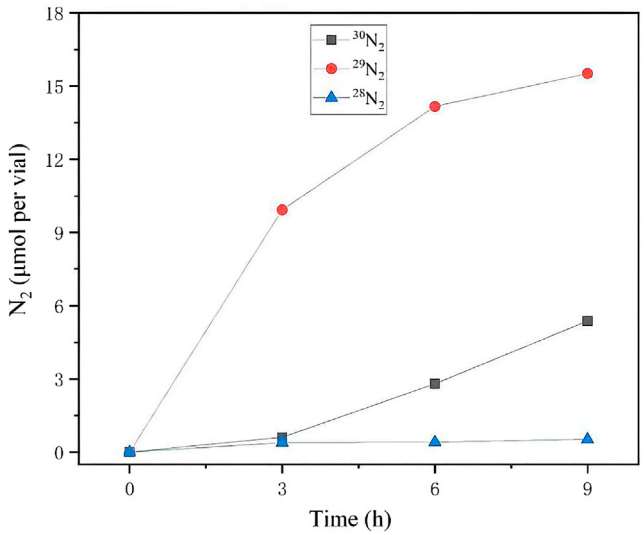

Figure 4. Time course of $^{30}N_2$, $^{29}N_2$, and $^{28}N_2$ generation from $^{15}NH_4^+$ and $^{14}NH_2OH$ in the anammox-CdS biohybrid system

light-driven conditions (NH_4^+ as the only substrate), 101 genes were upregulated and 248 were downregulated over 10 times generally (Data S1 and S2). For N metabolism and extracellular electron transfer, there were 10 genes upregulated shown in Table S2. Among the upregulated genes, the gene encoding hydroxylamine reductase (Hcp) was upregulated over 16-fold; in fact, it is a kind of ammonia oxidoreductase and can oxidize NH_3 to NH_2OH.[24] This finding positively supported our assumption that NH_2OH was the real intermediate in the photocatalytic-anammox process. Whereafter, the formed NH_2OH would be condensed with NH_4^+ to generate N_2H_4 by hydrazine synthase (HZS).[25] Eventually, N_2H_4 would be oxidized to N_2 by hydrozine dehydrogenase (HDH) and this step would release four low potential electrons to the quinone pool for the balance and the next cycle.[22] As there was no difference between the photocatalytic and normal anammox process in N_2H_4 generation and degradation, no pronounced discrepancy was monitored for the genes encoding HZS and HDH proteins in comparative transcriptomic analysis. On the other hand, there were 11 genes downregulated over 10 times for N metabolism, as shown in Table S3. Most downregulated genes were related to NO_3^- or NO_2^- conversion inside anammox bacteria. For instance, the gene encoding Nar/Nxr was downregulated, which was usually responsible for NO_3^- reduction to NO_2^-[26] or NO_2^- oxidation to NO_3^-.[27] Another example was the gene encoding Nir downregulated 2.2-fold, which was usually responsible for reducing NO_2^- to NO.[23] Generally, all the downregulated genes could be explained by the fact that neither NO_3^- nor NO_2^- was provided in our scenario.

Another important issue requiring to be addressed was the electron transfer from intracellular to extracellular photoexcited holes. In this case, there was several significant gene expression found in this electron transfer aspect. First, the genes encoding bc-1 was upregulated 2.9-fold (shown in Table S4), which was able to accept the electrons from N_2H_4 oxidation and transfer them into the cytoplasm.[28] Then the proton motive force would be generated and promote ATP synthesis.[28,29] Additionally, the gene encoding Fer located in the cytoplasm was upregulated as well, which was considered as an electronic shuttle as a non-heme electronic carrier.[10] Since no other related genes were found to be upregulated, it was proposed that the gene encoding Fer might play a role in electron transfer from the anammoxosome membrane to the inner membrane.[28,30] Furthermore, the cytochromes (kustd1708) or NADH-DU (both upregulated) were able to transfer electrons to the cytochrome (kustd1705, no obvious upregulated) located in the periplasm.[31–33] Subsequently, electrons were transferred to the cytochrome (kustd1710, upregulated) located on the outer membrane and would finally be captured by the photoexcited holes produced by CdS NPs. Previous studies reported that the porin-cytochrome proteins might have the function of extracellular electron transfer and be widespread in many phyla.[34,35] Notwithstanding, no porin-cytochrome proteins were found to be highly expressed in our study, which was different from the results of Shaw et al.[10] Further investigations must focus on the mechanism of electron transfer in the photocatalytic-anammox process.

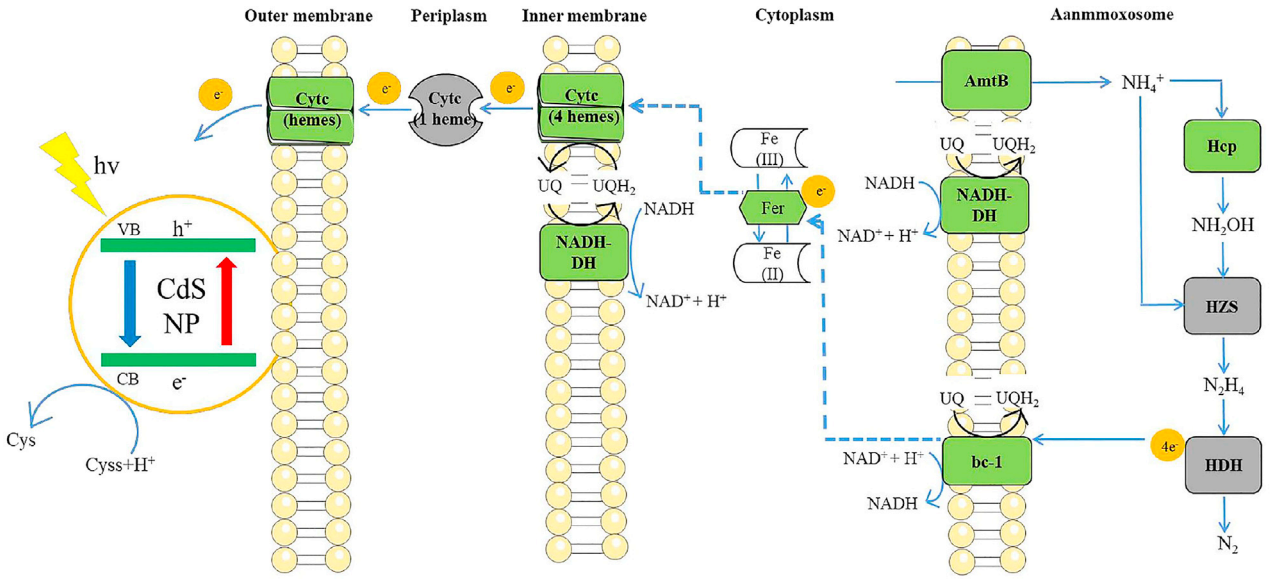

Figure 5. Mechanism diagram of photocatalytic oxidation of NH_4^+

Gene and gene clusters are shown in green if upregulated and the gray color corresponds to genes that are expressed under similar levels in both conditions (i.e., normal anammox process). Dashed lines represent the possible electron transfer process. The reactions are catalyzed by the Cytc (hemes): Membrane-anchored heme cytochrome *c*; Cyt *c* (1 heme): Mono-heme c-type cytochrome; Cyt *c* (4 hemes): Tetraheme c-type cytochrome; NADH-DU: NADH dehydrogenase; Fer: Similar to conserved hypothetical ferredoxin-like protein; AmtB: Ammonium transport protein; bc-1: Rieske/cytochrome *b* complex; Hcp: Hydroxylamine reductase; HZS: Hydrazine synthase; HDH: Hydrazine dehydrogenase.

Generally, the possible metabolism was expressed in Figure 5 and the suggested photosynthetic reaction for NH_4^+ oxidation was as following:

Electron-hole pair photogeneration:

$$hv \xrightarrow{CdS} h^+ + e^- \quad \text{(Equation 10)}$$

NH_4^+ oxidation to N_2:

$$2NH_4^+ + 6h^+ \rightarrow N_2 + 8H^+ \quad \text{(Equation 11)}$$

Cyss reduction to Cys:

$$Cyss + 2H^+ + 2e^- \xrightarrow{Anammox/CdS} 2Cys \quad \text{(Equation 12)}$$

Overall photosynthetic reaction:

$$2NH_4^+ + 3Cyss + 6hv \xrightarrow{Anammox/CdS} N_2 + 6Cys + 2H^+ \quad \text{(Equation 13)}$$

DISCUSSION

In fact, 1 h of solar irradiation could match our yearly global consumption demand, and sunlight present incomparable advantages in the renewable energy field.[36,37] The combination of inorganic semiconductors and non-photosynthetic microorganisms undoubtedly expanded the utilization of light energy, and might unfold the most salient attributes of semiconductors and microorganisms. Hitherto, all the constructed semiconductor-non-photosynthetic bacteria systems had mainly focused on the utilization of photoexcited electrons, which had been used for acetic acid,[11] H_2,[17,38] and NH_3[18] production from CO_2, H_2O, and N_2 reduction, respectively. None of the studies pays attention to the utilization of photoexcited holes by non-photosynthetic microbes. Consequently, it is the first time in this study to demonstrate the feasibility that photoexcited holes can be utilized by non-photosynthetic microbes to oxidize pollutants, e.g., NH_4^+. Other than photoexcited electrons, the applicability of photoexcited holes will further outspread the applicability of the semiconductors-bacterial hybrid system. Traditional wastewater treatment systems have been always deemed as energy-intensive. In addition, approximately 1000 km^3 of

municipal wastewater and 2.01 Gt municipal solid waste are released globally, which pose serious environmental and public health concerns especially in developing countries.[39] Undoubtedly, a huge amount of energy is required to implement hazard-free treatment. Our developed semiconductor-bacterial hybrid system, e.g., photoexcited holes utilization system, will provide an alternative to conventional wastewater treatment with much less energy consumption.

Besides semiconductors and vial microbes, another essential prerequisite for the semiconductor-bacterial hybrid system is the sacrifice reagent, which was cysteine with the function of quenching the photoexcited holes (h^+). For photosensitized bacteria, cysteine and ascorbic acid, as typical hole scavengers, usually limit the application scale-up.[40] Obviously, in order to ensure the economic viability and applicability of a semiconductors-bacterial hybrid system, the h^+ scavenger needs to be regenerated, low cost, and biocompatible.[40] In this scenario, we proved that photoexcited holes were utilized by non-photosynthetic bacteria to oxidize ammonium while cystine, as the sacrifice reagent, was used to capture photoexcited electrons and reduced to cysteine (Figure 2).

Forty-five years ago, Austrian phytochemist Broda[41] predicted the existence of two groups of missing autotrophs, e.g., phototrophy and chemolithrophys, which could use ammonium as an electron donor and NO_2^-/NO_3^- as electron acceptors to make dinitrogen gas. Twenty-seven years ago, Netherlandish microbiologists discovered and identified the missing chemolithotrophs as anammox bacteria.[42,43] In Broda's prediction, the phototrophy responsible for NH_4^+ oxidation with light as an energy source may be analogous to colored sulfur bacteria. While the above-mentioned phototrophy still remains undiscovered. In this study, we demonstrated that anammox bacteria could utilize photoexcited holes as electron acceptors to convert NH_4^+ to N_2 and grow. These results are believed to benefit the exploration and discovery of the missing phototrophy predicted by Broda in 1977. Simultaneously, NH_4^+ removal by the photocatalytic-anammox anammox is a superior alternative to traditional biological or non-biological NH_4^+ removal processed from water/wastewater with much less energy and cost consumption.

Conclusions

An anammox-semiconductor biohybrid system by coating biocompatible CdS on the anammox cell surface is constructed via facile strategies. The photoinduced holes from the CdS NPs could be utilized by anammox bacteria to convert NH_4^+ to N_2 without N_2O, NO_2^-, or NO_3^- accumulation. It can be proved that the anammox-CdS biohybrid system has photoautotrophic viability, and this study provides a promising and energy-efficient alternative for nitrogen removal from water/wastewater.

Limitations of the study

Although we constructed an anammox-CdS biohybrid system and utilized photoexcited holes as electron acceptors to directly oxide NH_4^+ to N_2, such a study can never cover all eventualities. Hence, future research will have to provide further evidence on the mechanism of photoexcited holes oxidation and the possibility of other bacteria using photoexcited holes oxidation.

STAR★METHODS

Detailed methods are provided in the online version of this paper and include the following:

- KEY RESOURCES TABLE
- RESOURCE AVAILABILITY
  - Lead contact
  - Materials availability
  - Data and code availability
- METHOD DETAILS
  - Preparation and characterization of cadmium sulfide (CdS)
  - Cadmium sulfide photocatalytic ability experiment
  - Cultivation of anammox biomass and its combination with CdS
  - Photocatalytic NH_4^+-N oxidation in the anammox-CdS biohybrid system
  - Bioanalysis in the anammox-CdS biohybrid system
  - The function of NO in photocatalytic reaction
  - ^{15}N isotope tracer experiment in the anammox-CdS biohybrid system
  - Metatranscriptomic sequencing analysis
- QUANTIFICATION AND STATISTICAL ANALYSIS

SUPPLEMENTAL INFORMATION

Supplemental information can be found online at https://doi.org/10.1016/j.isci.2023.106725.

ACKNOWLEDGMENTS

This work was financially supported by the National Key Research and Development Project (2019YFA0705804).

AUTHOR CONTRIBUTIONS

Conceptualization, M.G. and S.Q.; Methodology, M.G. and C.W.; Validation, C.W.; Formal Analysis, T.S.; Investigation, M.G. and S.Q.; Writing-Original Draft, M.G. and S.Q.; Visualization, C.W. and S.Q.; Supervision, C.W. and S.Q.

DECLARATION OF INTERESTS

The authors declare no competing interests.

Received: October 20, 2022
Revised: February 8, 2023
Accepted: April 20, 2023
Published: April 23, 2023

REFERENCES

1. Schaubroeck, T., De Clippeleir, H., Weissenbacher, N., Dewulf, J., Boeckx, P., Vlaeminck, S.E., and Wett, B. (2015). Environmental sustainability of an energy self-sufficient sewage treatment plant: improvements through DEMON and co-digestion. Water Res. *74*, 166–179. https://doi.org/10.1016/j.watres.2015.02.013.

2. Garrido-Amador, P., Kniaziuk, M., Vekeman, B., and Kartal, B. (2021). Learning from microorganisms: using new insights in microbial physiology for sustainable nitrogen management. Curr. Opin. Biotechnol. *67*, 42–48. https://doi.org/10.1016/j.copbio.2020.12.017.

3. Cruz, H., Law, Y.Y., Guest, J.S., Rabaey, K., Batstone, D., Laycock, B., Verstraete, W., and Pikaar, I. (2019). Mainstream ammonium recovery to advance sustainable urban wastewater management. Environ. Sci. Technol. *53*, 11066–11079. https://doi.org/10.1021/acs.est.9b00603.

4. Ravishankara, A.R., Daniel, J.S., and Portmann, R.W. (2009). Nitrous oxide (N_2O): the dominant ozone-depleting substance emitted in the 21st century. Science *326*, 123–125. https://doi.org/10.1126/science.1176985.

5. Van Dongen, U., Jetten, M.S., and van Loosdrecht, M.C. (2001). The Sharon-Anammox process for treatment of ammonium rich wastewater. Water Sci. Technol. *44*, 153–160. https://doi.org/10.2166/wst.2001.0037.

6. Strous, M., Van Gerven, E., Zheng, P., Kuenen, J.G., and Jetten, M.S. (1997). Ammonium removal from concentrated waste streams with the anaerobic ammonium oxidation (Anammox) process in different reactor configurations. Water Res. *31*, 1955–1962. https://doi.org/10.1016/S0043-1354(97)00055-9.

7. Haroon, M.F., Hu, S., Shi, Y., Imelfort, M., Keller, J., Hugenholtz, P., Yuan, Z., and Tyson, G.W. (2013). Anaerobic oxidation of methane coupled to nitrate reduction in a novel archaeal lineage. Nature *500*, 567–570. https://doi.org/10.1038/nature12375.

8. Van Loosdrecht, M.C.M., Hao, X., Jetten, M.S.M., and Abma, W. (2004). Use of anammox in urban wastewater treatment. Water Science and Technology. Water Supply *4*, 87–94. https://doi.org/10.2166/ws.2004.0010.

9. Lackner, S., Gilbert, E.M., Vlaeminck, S.E., Joss, A., Horn, H., and van Loosdrecht, M.C.M. (2014). Full-scale partial nitritation/anammox experiences-an application survey. Water Res. *55*, 292–303. https://doi.org/10.1016/j.watres.2014.02.032.

10. Shaw, D.R., Ali, M., Katuri, K.P., Gralnick, J.A., Reimann, J., Mesman, R., van Niftrik, L., Jetten, M.S.M., and Saikaly, P.E. (2020). Extracellular electron transfer-dependent anaerobic oxidation of ammonium by anammox bacteria. Nat. Commun. *11*, 2058–2069. https://doi.org/10.1038/s41467-020-16016-y.

11. Sakimoto, K.K., Wong, A.B., and Yang, P. (2016). Self-photosensitization of nonphotosynthetic bacteria for solar-to-chemical production. Science *351*, 74–77. https://doi.org/10.1126/science.aad3317.

12. Ye, J., Ren, G., Kang, L., Zhang, Y., Liu, X., Zhou, S., and He, Z. (2020). Efficient photoelectron capture by Ni decoration in methanosarcina barkeri-CdS biohybrids for enhanced photocatalytic CO_2-to-CH_4 conversion. iScience *23*, 101287–101313. https://doi.org/10.1016/j.isci.2020.101287.

13. Zhukovskyi, M., Tongying, P., Yashan, H., Wang, Y., and Kuno, M. (2015). Efficient photocatalytic hydrogen generation from Ni nanoparticle decorated CdS nanosheets. ACS Catal. *5*, 6615–6623. https://doi.org/10.1021/acscatal.5b01812.

14. Zhang, H., Liu, H., Tian, Z., Lu, D., Yu, Y., Cestellos-Blanco, S., Sakimoto, K.K., and Yang, P. (2018). Bacteria photosentitized by intracellular gold nanoclusters for solar fuel production. Nat. Nanotechnol. *13*, 900–905. https://doi.org/10.1038/s41565-018-0267-z.

15. Jin, S., Jeon, Y., Jeon, M.S., Shin, J., Song, Y., Kang, S., Bae, J., Cho, S., Lee, J.K., Kim, D.R., and Cho, B.K. (2021). Acetogenic bacteria utilize light-driven electrons as an energy source for autotrophic growth. Proc. Natl. Acad. Sci. USA *118*. e2020552118. https://doi.org/10.1073/pnas.2020552118.

16. Wei, W., Sun, P., Li, Z., Song, K., Su, W., Wang, B., Liu, Y., and Zhao, J. (2018). A surface-display biohybrid approach to light-driven hydrogen production in air. Sci. Adv. *4*, eaap9253z. https://doi.org/10.1126/sciadv.aap9253.

17. Martins, M., Toste, C., and Pereira, I.A.C. (2021). Enhanced light-driven hydrogen production by self-photosensitized biohybrid system. Angew. Chem. Int. Ed. Engl. *60*, 9055–9062. https://doi.org/10.1002/anie.202016960.

18. Wang, B., Xiao, K., Jiang, Z., Wang, J., Yu, J.C., and Wong, P.K. (2019). Biohybrid photoheterotrophic metabolism for significant enhancement of biological nitrogen fixation in pure microbial cultures. Energy Environ. Sci. *12*, 2185–2191. https://doi.org/10.1039/c9ee00705a.

19. Kuruvinashetti, K., and Kornienko, N. (2021). Pushing the methodological envelope in understanding the photo/electrosynthetic materials-microorganism interface. iScience *24*, 103049–103112. https://doi.org/10.1016/j.isci.2021.103049.

20. Ren, Z.Q., Yu, L.Q., Wang, H., Li, G.F., Zhang, L.G., Du, X.N., Huang, B.C., and Jin, R.C. (2022). Inorganic quantum dots-anammox consortia hybrid for stable nitrogen elimination under high-intensity solar-simulated irradiation. Water Res. *223*, 119033–119038. https://doi.org/10.1016/j.watres.2022.119033.

21. Cheng, L., Xiang, Q., Liao, Y., and Zhang, H. (2018). CdS-based photocatalysts. Energy Environ. Sci. *11*, 1362–1391. https://doi.org/10.1039/c7ee03640j.

22. Kartal, B., Maalcke, W.J., de Almeida, N.M., Cirpus, I., Gloerich, J., Geerts, W., Op den Camp, H.J.M., Harhangi, H.R., Janssen-Megens, E.M., Francoijs, K.J., et al. (2011). Molecular mechanism of anaerobic ammonium oxidation. Nature *479*, 127–130. https://doi.org/10.1038/nature10453.

23. Oshiki, M., Ali, M., Shinyako-Hata, K., Satoh, H., and Okabe, S. (2016). Hydroxylamine-dependent anaerobic ammonium oxidation (anammox) by "Candidatus Brocadia sinica". Environ. Microbiol. *18*, 3133–3143. https://doi.org/10.1111/1462-2920.13355.

24. Schomburg, D., and Schomburg, I., eds. (2005). Hydroxylamine reductase. In Springer Handbook of Enzymes, *24*. https://doi.org/10.1007/3-540-37662-3_79.

25. Dietl, A., Ferousi, C., Maalcke, W.J., Menzel, A., de Vries, S., Keltjens, J.T., Jetten, M.S.M., Kartal, B., and Barends, T.R.M. (2015). The inner workings of the hydrazine synthase multiprotein complex. Nature *527*, 394–397. https://doi.org/10.1038/nature15517.

26. Ruiz, B., Le Scornet, A., Sauviac, L., Rémy, A., Bruand, C., and Meilhoc, E. (2019). The nitrate assimilatory pathway in sinorhizobium meliloti: contribution to NO production. Front. Microbiol. *10*, 1526–1612. https://doi.org/10.3389/fmicb.2019.01526.

27. Schomburg, D., and Schomburg, I., eds. (2005). Ferredoxin-nitrate reductase. In Springer Handbook of Enzymes, *24*. https://doi.org/10.1007/3-540-37662-3_78.

28. De Almeida, N.M., Wessels, H.J., De Graaf, R.M., Ferousi, C., Jetten, M.S.M., Keltjens, J.T., and Kartal, B. (2016). Membrane-bound electron transport systems of an anammox bacterium: a complexome analysis. Biochim. Biophys. Acta *1857*, 1694–1704. https://doi.org/10.1016/j.bbabio.2016.07.006.

29. Akram, M., Dietl, A., Mersdorf, U., Prinz, S., Maalcke, W., Keltjens, J., Ferousi, C., De Almeida, N.M., Reimann, J., Kartal, B., et al. (2019). A 192-heme electron transfer network in the hydrazine dehydrogenase complex. Sci. Adv. *5*, eaav4310-7. https://doi.org/10.1126/sciadv.aav4310.

30. Kartal, B., de Almeida, N.M., Maalcke, W.J., Op den Camp, H.J.M., Jetten, M.S.M., and Keltjens, J.T. (2013). How to make a living from anaerobic ammonium oxidation. FEMS Microbiol. Rev. *37*, 428–461. https://doi.org/10.1111/1574-6976.12014.

31. Shi, L., Dong, H., Reguera, G., Beyenal, H., Lu, A., Liu, J., Yu, H.Q., and Fredrickson, J.K. (2016). Extracellular electron transfer mechanisms between microorganisms and minerals. Nat. Rev. Microbiol. *14*, 651–662. https://doi.org/10.1038/nrmicro.2016.93.

32. Luo, S., Guo, W., Nealson, K.H., Feng, X., and He, Z. (2016). C-13 pathway analysis for the role of formate in electricity generation by Shewanella oneidensis MR-1 using lactate in microbial fuel cells. Sci. Rep. *6*, 20941–20948. https://doi.org/10.1038/srep20941.

33. Beckwith, C.R., Edwards, M.J., Lawes, M., Shi, L., Butt, J.N., Richardson, D.J., and Clarke, T.A. (2015). Characterization of MtoD from Sideroxydans lithotrophicus: a cytochrome c electron shuttle used in lithoautotrophic growth. Front. Microbiol. *6*, 332–338. https://doi.org/10.3389/fmicb.2015.00332.

34. Liu, Y., Wang, Z., Liu, J., Levar, C., Edwards, M.J., Babauta, J.T., Kennedy, D.W., Shi, Z., Beyenal, H., Bond, D.R., et al. (2014). A trans-outer membranes porin-cytochrome protein complex for extracellular electron transfer by Geobacter sulfurreducens PCA. Environ. Microbiol. Rep. *6*, 776–785. https://doi.org/10.1111/1758-2229.12204.

35. Shi, L., Fredrickson, J.K., and Zachara, J.M. (2014). Genomic analyses of bacterial porin-cytochrome gene clusters. Front. Microbiol. *5*, 657–710. https://doi.org/10.3389/fmicb.2014.00657.

36. Lewis, N.S. (2016). Research opportunities to advance solar energy utilization. Science *351*, aad1920. https://doi.org/10.1126/science.aad1920.

37. Cestellos-Blanco, S., Zhang, H., Kim, J.M., Shen, Y.x., and Yang, P. (2020). Photosynthetic semiconductor biohybrids for solar-driven biocatalysis. Nat. Catal. *3*, 245–255. https://doi.org/10.1038/s41929-020-0428-y.

38. Wang, B., Zeng, C., Chu, K.H., Wu, D., Yip, H.Y., Ye, L., and Wong, P.K. (2017). Enhanced biological hydrogen production from Escherichia coli with surface precipitated cadmium sulfide nanoparticles. Adv. Energy Mater. *7*, 1700611–1700710. https://doi.org/10.1002/aenm.201700611.

39. WWAP (2017). The United Nations World Water Development Report 2017. Wastewater: The Untrapped Resource (UNESCO).

40. Blanco-Cestellos, S., Kim, J.M., Watanabe, N.G., Chang, R.R., and Yang, P.D. (2021). Molecular insights and future frontiers in cell photosensitization for solar-driven CO_2 conversion. iScience *13*, 1–2. https://doi.org/10.1016/j.isci.2021.102952.

41. Broda, E. (1977). Two kind of missing lithotrophs missing in nature. Z. Allg. Mikrobiol. *17*, 491–493. https://doi.org/10.1002/jobm.3630170611.

42. Mulder, A., Graaf, A., Robertson, L.A., and Kuenen, J.G. (1995). Anaerobic ammonium oxidation discovered in a denitrifying fluidized bed reactor. FEMS Microbiol. Ecol. *16*, 177–184. https://doi.org/10.1016/0168-6496(94)00081-7.

43. Strous, M., Fuerst, J.A., Kramer, E.H., Logemann, S., Muyzer, G., van de Pas-Schoonen, K.T., Webb, R., Kuenen, J.G., and Jetten, M.S. (1999). Missing lithotroph identified as new planctomycete. Nature *400*, 446–449. https://doi.org/10.1038/22749.

44. Dumbrava, A., Prodan, G., Berger, D., and Bica, M. (2015). Properties of PEG-capped CdS nanopowders synthesized under very mild conditions. Powder Technol. *270*, 197–204. https://doi.org/10.1016/j.powtec.2014.10.012.

STAR★METHODS

KEY RESOURCES TABLE

REAGENT or RESOURCE	SOURCE	IDENTIFIER
Bacterial and virus strains		
Anammox bacteria	A lab-scale Up-flow Anaerobic Sludge Bed (UASB) reactor	N/A
Candidatus Kuenenia stuttgartiensis	Anammox bacteria	N/A
Chemicals, peptides, and recombinant proteins		
2-phenyl-4,4,5,5,-tetramethylimidazoline-1-oxyl-3-oxide (PTIO)	Macklin	P838429; CAS: 18390-00-6
$^{15}NH_4Cl$ (^{15}N, 99%)	Cambridge Isotope Laboratories	NLM-467-5
Deposited data		
Raw and analyzed data	This paper	SRR23019768
Experimental models: Organisms/strains		
Anammox bacteria	A lab-scale Up-flow Anaerobic Sludge Bed (UASB) reactor	N/A
Candidatus Kuenenia stuttgartiensis	Anammox bacteria	N/A
Oligonucleotides		
Probes: EUB338 (5′-FAM-GCTGCCTCCCGTAGGAGT-3′) and Amx0368 (5′-CCTTTCGGGCATTGCGAA-3′)	This paper	N/A
Primers: 341F (CCTACGGGNGGCWGCAG) and 805R (GACTACHVGGGTATCTAATCC)	This paper	N/A
Primers: Amx809F (GCCGTAAACGATGGGCACT) and Amx1066R (AACGTCTCACGACACGAGCTG)	This paper	N/A
Software and algorithms		
Image-Pro Plus	This paper	N/A

RESOURCE AVAILABILITY

Lead contact

Further information and requests for resources should be directed to and will be fulfilled by the lead contact, Sen Qiao (qscyj@mail.dlut.edu.cn).

Materials availability

This study did not generate new unique materials.

Data and code availability

- All data produced in this study are included in the published article and its supplementary information and supplementary data, or are available from the lead contact upon request.
- This paper does not report original code.
- Any additional information required to reanalyze the data reported in this paper is available from the lead contact upon request.

METHOD DETAILS

Preparation and characterization of cadmium sulfide (CdS)

The method for preparing CdS nanoparticles was roughly the same as that described by Dumbrava et al.[44] The CdS nanoparticles were prepared by the grinding method. Firstly, $Cd(CH_3COO)_2 \cdot 2H_2O$ (2.66 g) was dissolved in 1.75 mL polyethylene glycol (PEG 400). Then, CH_3CSNH_2 (0.75 g) was added and the mixture

was grinded until completely dissolved. The mixed solution was intermittently grinded and placed overnight to obtain a uniform yellow paste, stirred with ultrapure water for 10 min, finally washed with ultrapure water several times, dried and grinded to obtain orange-yellow powders. XRD was used to identify the crystalline properties (the 2θ range of 20°–90°) and the crystal form of the produced orange-yellow CdS nanoparticles. XPS was utilized to investigate the constituent elements, valence state and relative content of substances. The UV-Vis absorption spectrum was used to detect the CdS absorption spectrum in the range of 300–800 nm. HR-SEM, HAADF TEM and TEM were used to observe the surface morphology of anammox bacteria combined with CdS nanoparticles, and EDS was used to detect the element content and distribution on the surface of anammox bacteria.

Cadmium sulfide photocatalytic ability experiment

The experiments demonstrating the photocatalytic ability of CdS were consistent with the method used by Jin et al.[15] 100 mg of CdS nanoparticles were added to Congo Red solution (200 mL, 30 mg/L), and stirred for 30 min under dark conditions to reach adsorption-desorption equilibrium. Then the solution surface was irradiated with a halogen lamp at a distance of 15 cm for one hour, and sample was abstracted at 0, 15, 30, 45, and 60 min. The concentration of Congo Red in the solution was measured using the UV-Vis absorption spectrum (UV-Vis, UH41500304042501, Hitachi, Japan) to scan the full-wave. The ultrapure water was the reference solution. The UV absorption spectrum of Congo Red solutions was scanned in the range of 300–800 nm, and the absorption peaks of Congo Red appeared at 497 and 347 nm.

Cultivation of anammox biomass and its combination with CdS

Anammox biomass was enriched and cultivated by a lab-scale Up-flow Anaerobic Sludge Bed (UASB) reactor. The reactor adopted a continuous water inlet and outlet method, keeping the temperature constant at 35 ± 2°C. The composition of the culture medium was shown in Table S4. The concentration range of ammonia nitrogen and nitrite nitrogen were NH_4^+-N (50-100 mg-N/L) and NO_2^--N (66-132 mg-N/L), respectively (NO_2^--N/NH_4^+-N about 1.32, in line with the theoretical ratio of the normal anammox reaction). The hydraulic retention time was set as 4 h.

5 g wet weight of anammox biomass was adopted from the reactor, washed several times with phosphate buffered solution (PBS) solution, and added into an experimental vial. The vial contained 100 mL of the culture medium without NH_4^+-N and NO_2^--N, sparged with helium to ensure anaerobic conditions in the vial. Then 0.25 g of CdS nanoparticles were put into the vial, fully contacted the anammox biomass and incubated in a constant temperature shaker at 35°C with a speed of 100 rpm for 24 h. At this time, the CdS nanoparticles had been bound to the surface of anammox biomass to form the anammox-CdS biohybrid system.

Photocatalytic NH_4^+-N oxidation in the anammox-CdS biohybrid system

After constructing the anammox-CdS biohybrid system, the supernatant of the vial was poured out and then the vial was added 100 mL the medium containing 25 mg-N/L NH_4^+-N, and 0.1 g cystine. Helium gas was sparged to remove the possible remained oxygen before refilling the medium, and the experimental vial was irradiated with a LED lamp (490 nm) at a constant temperature of 35°C. The control group without anammox biomass was the non-biological control group, the one without CdS nanoparticles was the positive control group, and the one without LED light was the negative control group. The other conditions of the control groups were kept as the same with experimental groups. The qualities of NH_4^+-N, NO_2^--N and NO_3^--N were determined by an ion chromatograph (DIONEX ICS, Thermo Fisher, USA); the quality of cysteine was detected by high performance liquid chromatography (HPLC, LC-20A, SHIMADZU, Japan); the qualities of N_2 and N_2O were detected by gas chromatograph (GC7900, Tianmei, China).

Bioanalysis in the anammox-CdS biohybrid system

1 g wet weight of anammox biomass was adopted from the reactor, washed several times with PBS solution, and sent to Shanghai Bioengineering Company, to perform fluorescence *in situ* hybridization (FISH) detection. Samples of anammox biomass were fixed, hybridized and eluted, and further observed and imaged by a laser scanning confocal microscope (Confocal laser scanning microscope, Olympus, Japan). The collected images were counted using Image-Pro Plus software. EUB338 (5′-FAM-GCTGCCTCCCGTAG GAGT-3′) and Amx0368 (5′-CCTTTCGGGCATTGCGAA-3′) were used as probes for total bacteria and anammox bacteria, respectively.

Samples of anammox biomass in the UASB reactor were washed several times with PBS solution and sent to Shanghai Bioengineering Company, to conduct 16S rDNA microbial classification and sequencing to analyze the microbial community. DNA extraction, PCR amplification and sequencing procedures were as follows. DNA extraction kit (OMEGA EZNATM Mag-Bind Soil DNA Kit, Norcross, GA, U.S.) was used to extract the total DNA of the microbial community, and PCR amplification was carried out after detection of the purity and concentration of the extracted DNA. The corresponding region of primers was 16S V3-V4 region that the upstream primer was 341F (CCTACGGGNGGCWGCAG) and the downstream primer was 805R (GACTACHVGG GTATCTAATCC). The amplified PCR was identified, purified and quantified, and then a library was constructed and sequenced by Illumina. OTU clustering and taxonomic analysis were performed on the data.

The real-time fluorescent quantitative PCR technology (qPCR, LightCycler480 I, Rotkreuz, Switzerland) was used to quantitatively analyze the abundance of the anammox bacteria without CdS and the biomass in the anammox-CdS biohybrid system. During the stable period, 5 g wet weight of anammox biomass was extracted for photocatalytic NH_4^+-N oxidation experiment, as described above. The control group was to run the normal anammox reaction (with NH_4^+ 25 mg-N/L and NO_2^- 33 mg-N/L). On the 7th day of the experiment, the biomass in the experimental group and the control group were centrifuged several times with PBS solution (10000 rpm, centrifugation for 5 min), and 1g wet weight biomass were sampled and quickly frozen with liquid nitrogen for 1 min, and sent to Shanghai Bioengineering Company for analysis. The primer sequence of the target gene was shown in Table S5.

The function of NO in photocatalytic reaction

The anammox-CdS biohybrid system was incubated with NH_4^+-N of 25 mg-N/L, PTIO (2-phenyl-4,4,5,5-tetramethylimidazoline-3-oxo- 1-Oxygen) of 500 mg/L co-cultivation for 9 h. As NO scavenger,[10] PTIO can react with NO to generate PTI (2-(4-carboxyphenyl)-4,4,5,5-tetramethylimidazoline-1-oxyl) derivatives, and simultaneously produce nitrite and nitrate, thereby eliminating NO. In order to explore the effects of PTIO, two control experiments were conducted in parallel. One control was the same anammox-CdS biohybrid system (NH_4^+-N of 25 mg/L) only without PTIO addition. The other control, with PTIO addition, utilized NH_4^+ (25 mg/L) and NO_2^- (33 mg/L) as the substrate to run normal anammox reaction. Other components of the medium were the same as those described in part of photocatalytic NH_4^+-N oxidation experiment.

^{15}N isotope tracer experiment in the anammox-CdS biohybrid system

The ^{15}N stable isotope tracer experiment was used to explore the pathway of NH_4^+-N conversion in the anammox-CdS biohybrid system. After anammox biomass was combined with the CdS nanoparticles, the supernatant was poured out, and the labeled $^{15}NH_4Cl$ of 25 mg-N/L (Cambridge Isotope Laboratories, Trading Company, USA), 0.1 g cystine were added to the vial along with 100 mL medium incubated for 9 h (sparged with helium to ensure anaerobic conditions in the vial), and with gas sample analysis every 3 h. The concentration of $^{28}N_2$, $^{29}N_2$, $^{30}N_2$, ^{14}NO, ^{15}NO, $^{28}N_2O$, $^{29}N_2O$ and $^{30}N_2O$ were measured by a gas chromatography-mass spectrometer (GCMS-QP, SHIMADZU, Japan).

To exploit the real intermediate product during photocatalytic NH_4^+-N oxidation process, the anammox-CdS biohybrid system was incubated with $^{15}NH_4Cl$ of 25 mg-N/L (Cambridge Isotope Laboratories, Trading Company, USA) and $^{14}NH_2OH$ of 12.5 mg-N/L for 9 h, and extracted the headspace gas every 3 h to detect the content of $^{30}N_2$, $^{29}N_2$ and $^{28}N_2$ produced by the gas chromatography-mass spectrometer (GCMS-QP, SHIMADZU, Japan).

Metatranscriptomic sequencing analysis

Possible metabolic pathways for photocatalytic NH_4^+-N oxidation was exploited through metatranscriptomic sequencing analysis. The anammox-CdS biohybrid system (the experimental group) was cultured for 7 days and the biomass samples were washed three times with PBS, and 3 g wet weight of anammox biomass was quickly frozen in liquid nitrogen. The control group samples were taken from the lab-scale UASB anammox reactor with NH_4^+-N and NO_2^--N as the substrate, respectively. The treatment method was the same as the experimental group. Samples of the experimental group and the control group were sent to Shanghai Bioengineering Company for further analysis.

QUANTIFICATION AND STATISTICAL ANALYSIS

All the results were the average of tri-measurements with standard error.